



Propagation of Microcracks in Bovine Osteonal Cortical Bone

Ahmad Raeisi Najafi^a, Kaveh PourAkbar Saffar^{b‡}, Ahmad Reza Arshi^c, Erfan Mallakin^c, Hamid Reza Katouzian^c, Mohammad Reza Eslami^d, Manssour H. Moeinzadeh^a

a Department of Industrial and Enterprise Systems Engineering, University of Illinois at Urbana-Champaign, IL, USA

b Department of Mechanical and Manufacturing Engineering, University of Calgary, AB, Canada

c Department of Biomedical Engineering, Amirkabir University of Technology, Tehran, Iran

d Department of Mechanical Engineering, Amirkabir University of Technology, Tehran, Iran

Bone toughening and fracture mechanics are an important area of study for medical scientists seeking to predict and prevent fracture risk, and for engineers interested in designing novel, biologically-inspired materials. This paper reports on the effect of internal bone microstructure upon microcrack propagation trajectory in bovine osteonal cortical bone. A two-dimensional micromechanical fibre-reinforced composite materials model was generated using the finite element method. Interstitial tissue was modeled as a matrix, osteons as fibres, and the 'cement line' as an interface between osteons and interstitial tissue. Fracture tests on compact tension samples of bovine femur were performed and compared to modeling predictions. Micrographs of fracture surfaces were obtained using scanning electron microscopy. Results show that cortical bone microcrack propagation is greatly influenced by osteonal density, suggesting bone resistance to fracture can be predicted, at least in part, by quantification of osteonal density.

KEYWORDS: Osteonal cortical bone; fracture; microcrack propagation; finite element; scanning electron microscopy

COPYRIGHT: © 2011 Raeisi Najafi *et al.* This is an open-access article distributed under the terms of the Creative Commons Attribution License, which permits unrestricted use, distribution, and preproduction in any medium, provided the original author and source are credited.

Bone is a multi-scale hierarchical structure composed of collagen, water, and mineral nanoparticles. Arrangements of these components into different functional units, creates a light but tough structure that is multi-functional and able to adapt to diverse mechanical environments [1]. Bone mass or bone mineral density is the parameter that is most commonly used to determine bone deterioration with age and to predict bone susceptibility to fracture [1-3]. However, recent research clearly shows that reduced bone mineral density is not the sole factor in increased fracture risk [4-8]. A more complete understanding of bone fracture can be achieved by

studying active fracture/ bone toughening mechanisms at different levels of its structure [1,2, 9-12]. Intrinsic toughening mechanisms such as molecular uncoiling, intermolecular sliding, microcracking, and fibrillar sliding, act at a submicrostructural level to enhance structural resistance to the initiation and growth of cracks. At a microstructural level, extrinsic shielding mechanisms such as crack deflection and twisting, uncracked ligament bridging, collagen fibril bridging, and constrained microcracking occur and improve bone toughness by shielding the crack tip from applied driving force [1,4,5]. Previous bone fracture studies show that active extrinsic shielding mechanisms at the microstructural level influence toughness of cortical bone by changing crack growth trajectory [5].

Osteons are the functional units of compact (cortical) bone. They are separated from one

[‡]Correspondence: kpourakb@ucalgary.ca

Received: 29 September 2010; Accepted: 01 February 2011

another by interstitial tissue. The interface between the osteons and interstitial tissue is a third type of tissue called the cement line. The osteonal (Haversian) cortical bone can be modelled as a biological fibre–ceramic matrix composite material [12,13].

There are different types of cavities and sites of weakness within bone that provide sites for crack initiation. These include the Haversian canals and the weak interfaces between lamellae [14]. Osteons can act as a barrier to limit the growth of microcracks [14-17]. Previous work by our group modelled human osteonal cortical bone at a microstructural level and analyzed the effect of this microstructure upon microcrack growth path [18]. This model showed that osteons cause deflections in microcrack path. Furthermore, a multi-osteonal model showed that microcracks slow down and eventually come to a complete halt in the boundary of osteons at the cement line, when they enter an area of high osteon density [18]. Both of these toughening mechanisms increase bone resistance to fracture.

Based on this previous work, we sought to evaluate the effect of osteon density on fracture phenomena in bovine osteonal cortical bone. Microcrack propagation was modelled using the finite element method (FEM), based on previously reported values for elastic moduli of bovine osteonal cortical bone. Modeling outcomes were compared to fracture tests and scanning electron microscopy (SEM) micrographs of real bovine osteonal cortical bone.

Materials and Methods

Finite Element Model

A two dimensional plane strain model was used to model the microstructure of compact bone. Osteons were modeled as hollow fibres and the interstitial tissue, which fills the space between the osteons, was modeled as a matrix (fig. 1). The cement line interface between the osteon and interstitial tissues was also included (fig. 1). In this model, all constituents were taken to be homogeneous and isotropic in planes perpendicular to the axis of bone, and perfect bonding was assumed between the interfaces.

Mechanical properties of bone constituents are heavily influenced by various factors such as bone type, anatomical location, age, gender and state of health. As such, average values were drawn from previously published reports. The elastic moduli in wet bovine diaphyseal femoral bone has been reported to be 21.1 ± 2.0 GPa in osteonal and 25.1 ± 1.6 GPa in interstitial lamellae [19]. Values of 21 GPa for osteonal effective elastic modulus (E_o) and 25

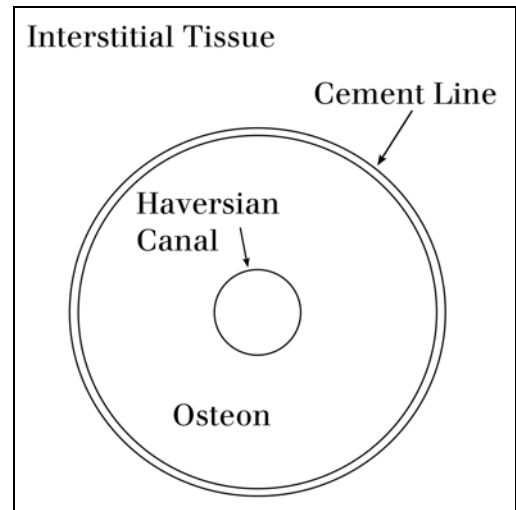


Figure 1. Fibre-reinforced composite micromechanical model for the Haversian cortical bone

GPa for interstitial tissue elastic modulus (E_i) were thus adopted for the evaluation of the effect of mechanical properties upon microcrack behavior. Poisson's ratio for the osteon and the interstitial bone was assumed to be 0.3 [20].

The mechanical characteristics of the cement line tissue have also been variously reported. Some reports consider it softer than the surrounding tissues (e.g. [21]). Other researchers such as Curry suggest a more mineralized structure and thus a higher modulus of elasticity [22]. In this paper, following the suggestion made by Advani *et al.* [23], the simulation was repeated twice for values of 10 and 30 GPa (E_c) with the assumed Poisson ratio of 0.3 [20].

Quantitative analyses of osteons and Haversian canals have also been reported: Secondary osteon size and osteon density are found to vary in different animals and anatomical locations [24-29]. Furthermore, these parameters vary with age [24,26]. Microscopic observation shows that osteons and Haversian canals are elliptical in bovine femurs [24], with various reported values for diameters. Diameters of osteons are in the range of 52-297 μm and Haversian canal diameters are in the range of 9-45 μm in bovine femurs [24,27]. In this study, osteons and Havesian canals were modeled as cylinders with diameters of 100 μm and 20 μm , respectively. Osteon density was assumed to be in the range of 20-30 per mm^2 and a thickness of 1 μm was assumed for the cement lines.

Fracture analysis was performed using Franc2D and the program Casca version 1.4 was used to produce a two-dimensional mesh. Two types of triangular elements with six nodes and square elements with eight nodes were used for making the

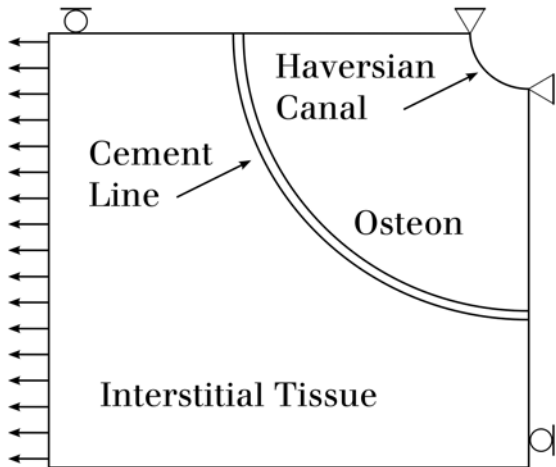


Figure 2. Quarter model boundary condition for FEM fracture analysis

finite element mesh. As shown in **figure 2**, the nodal displacements along the boundary nodes were coupled so that the boundaries remain straight and parallel to their initial states during the deformation period [18]. Normal stress in the boundary was taken to be 15 MPa in the mid-diaphysis of long bone [20].

To study the effect of bone microstructure and mechanical material properties on microcrack propagation trajectory, two paradigms were investigated: An edge crack interacting with a single osteon, and an internal crack interacting with an arrangement of multiple osteons in interstitial tissue. Here maximum hoop stress was adopted to determine the propagation direction. Hoop stress (σ_θ) is determined around the crack tip on the circumference of a constant radius circle. The microcrack propagation is in the direction that is associated with maximum hoop stress. The corresponding mathematical description is provided by **equations (1) and (2)** [20].

$$\frac{\partial \sigma_\theta}{\partial \theta} = 0 \quad (\text{eq. 1})$$

$$\frac{\partial^2 \sigma_\theta}{\partial \theta^2} < 0 \quad (\text{eq. 2})$$

Experimental Tests

Compact bone samples were obtained from bovine femurs within 24 hours of slaughter. Distal and proximal ends were removed and the remaining section was divided into six portions, each approximately 5 cm long. The portions were cleaned of any soft tissues in order to obtain 23 standard

(ASTM-E399) compact tension (CT) samples. **Figure 3** shows a schematic illustration of the direction of a CT sample prepared from a bovine femur diaphysis.

The specimens were machined to an approximate size of 27.5 mm x 23.5 mm with a thickness of 4-7 mm. A chevron notch was also machined on the transverse bone axis. A razor blade was then used to introduce a pre-crack on the notch. The specimens were kept moist using saline solution during machining and storage. Samples were mounted on a dynamic testing machine (Zwik/Roell 321 htm 125) using specially prepared fixtures. Slow fracture occurred during tension loading at a crosshead rate of 0.005 mm/sec. After fracture testing, samples were stored in 3% hydrogen peroxide at room temperature for 48 hours. Samples were dehydrated by placing them in 37% ethanol followed by 100% ethanol for 4 and 8 hours, respectively. The samples were subsequently air-dried. Fractured samples were gold coated at the pressure of 0.001 mbar and the SEM produced photographs of the fracture surfaces. The ensuing fractographical results of fracture surfaces were used to acquire information on microcrack propagation trajectory.

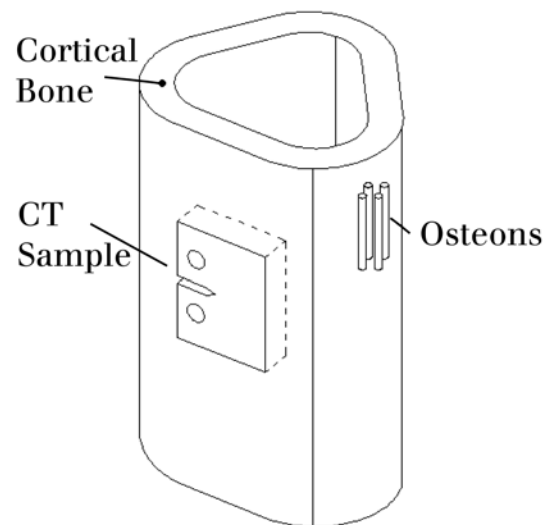


Figure 3. Schematic illustration of location of the CT sample from bovine femur diaphysis

Results

Finite Element Model

In fracture propagation analysis, the edge microcrack was situated in a vertical direction to the loading (**fig. 4a**). Data in **figures 4b and 4c** show that within the adopted range of elastic moduli for different tissues, the microcrack trajectories were deviated from the osteon.

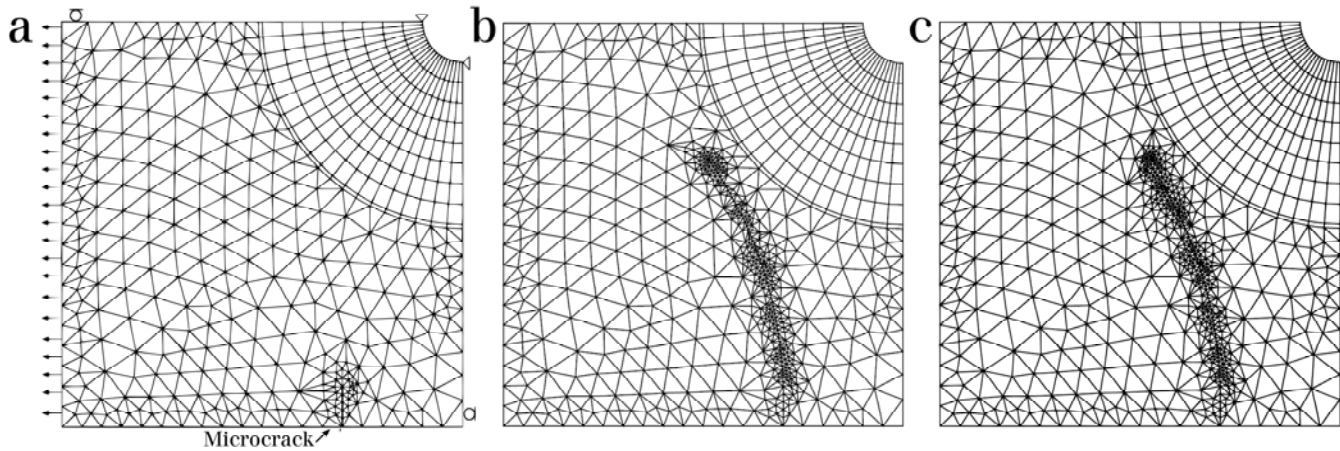


Figure 4. Edge microcrack interacting with a single osteon under tension a) Primary microcrack, b) Propagation trajectory, $E_c=50$ GPa, c) $E_c=10$ GPa

The model was further developed by placing a number of osteons in the interstitial tissue region. Resultant data show that the microcracks do not propagate through the interstitium when the distance between osteons is very small (fig. 5).

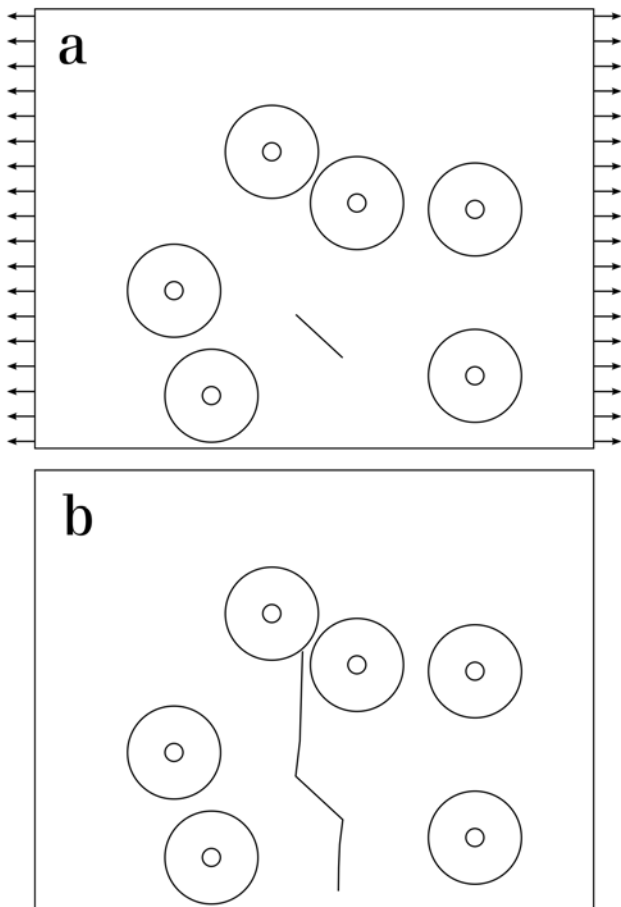


Figure 5. Internal microcrack interacting with multiple osteons, a) Primary microcrack, b) Propagation of microcrack

Fracture Test

A fractured sample and the fracture surface SEM photographs are shown in figure 6. The pre-crack orientation is perpendicular to longitudinal bone axis (figure 6a). The data show deviation of the microcrack from the osteon and microcrack halting at the cement line boundary. The first microcrack of approximately 400 μm (microcrack (1), figure 6b), continued to propagate after deviating in the vicinity

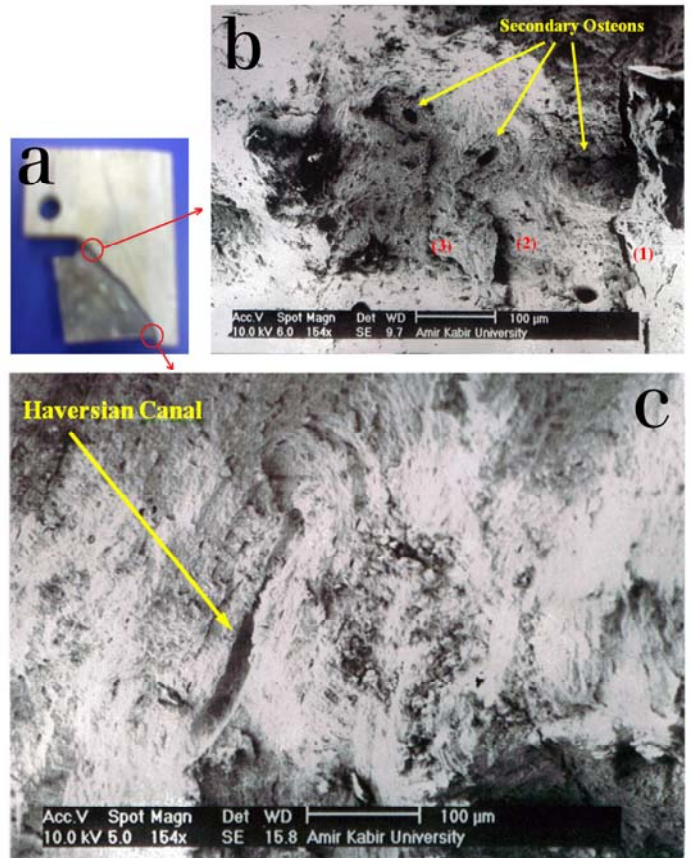


Figure 6. a) Fractured CT sample, b) SEM of fracture surface at main crack initiation region, c) SEM of surface at fractured end

of the osteons. Microcracks (2) and (3) also came to a halt once they reach the osteons. Such behavior indicates that in regions where the osteons are closely situated, the microcracks stop at the cement line boundary as they cannot infiltrate the space between osteons. As expected, during growth, the main crack deviates in a way that propagates in between osteons and in parallel with their longitudinal direction. This phenomenon is clearly shown in **figure 6c**. In this figure, a Haversian canal can be observed parallel to the fracture surface. This view does not show the cross section of the system of secondary osteons. This demonstrates that the main crack grows parallel to the direction of osteons.

The SEM photograph of **figure 7** represents an inter-lamellar level study of fracture surface. Individual lamellae layers are identified by the label 'L' in the picture. Delamination is also quite evident in this figure. Chunks of lamellae, as shown by arrows in this figure, are also detached. Inter-laminar fibres connecting the separating lamellae layers are shown by dashed line arrows. There were also a number of holes, indicated by the label 'H' in the same figure, from which microcrack initiation took place.

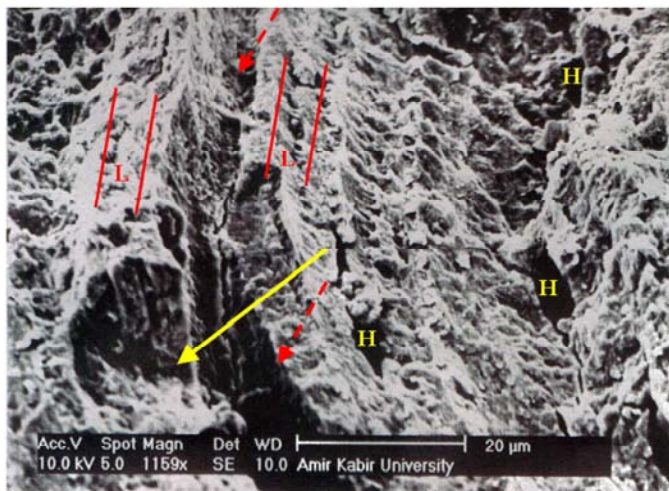


Figure 7. Detail of regions between lamellae (L) and inter-laminar fibres (dashed arrows). Separation of a mass of lamellae (solid arrow) and a number of holes (H) can also be observed.

Discussion

Here we report on the fracture micromechanics of osteonal cortical bone and the effects of the material properties, morphology and microstructure upon fracture phenomenon. In the presented model, all constituents (interstitial tissue, osteon and cement line) were considered homogeneous and isotropic in planes perpendicular to the bone's axis. Microcracks occur in the microcrack zone at the crack tip region, but in different orientations not necessarily in the

plane of the main crack [18]. They are assumed to be situated within the interstitial tissue in accordance with the results of previously reported *in vivo* experiments [14,30]. Two phenomena are not considered in this model, namely cement line debonding and osteon pullout. The model also represents a plane strain condition. In long bone, longitudinal dimension is quite large in comparison to its diameter. The loading in the current model occurs in a perpendicular direction to the longitudinal axis. This leads to consideration of plane strain condition in the 2D model of cortical bone during lateral loading. In fact, in cortical bone, under axial loading, the microcracks are expected to grow in the transverse direction due to lateral strains which are caused by the longitudinal strains (Poisson effect) [18].

The results are a clear indication of the effect of microstructure heterogeneity upon Haversian cortical bone fracture behaviour. The effect of osteons on microcrack propagation depends on the mechanical properties of various microstructural tissues, as suggested by other experimental and theoretical reports [13,15,31]. Experimental results indicate mechanical properties associated with the osteons and interstitial tissues vary with age [32,33], with a severe effect on the bone fracture mechanics [13,31]. It could also be argued that the underlying reason for an increased susceptibility of bone to fracture is due to changes in the mechanical properties of different tissues in the bone.

The principle finding of this study was that microcrack propagation trajectory is influenced by the osteonal cortical bone microstructure [14,15,34]. SEM photographs of fracture surfaces and FEM results were in close agreement. Results indicate that the microcracks are deviated as they approach the osteons. The microcrack path deviation is however dependent upon such parameters as osteon density. When the distance between osteons is small and the osteon density is higher, then microcrack propagation cannot follow a trajectory between the osteons and stops at the cement line boundary. It could therefore be concluded that osteons act as a barrier against microcrack propagation, as shown by microcracks (2) and (3) in **figure 6**, which is also suggested by the FEM simulation results shown in **figure 5**. In bone tissue, short cracks are therefore encountered more frequently than long cracks [35]. Other researchers have also reported similar observations in experimental studies [14,15]. Experiments carried out by O'Brien *et al.* [14], also suggest that microcracks shorter than 300 µm are deviated in the vicinity of the osteon, or are stopped at the cement line. In effect, although the osteons reduce bone

strength, they act as a barrier to microcrack growth [14,15,36] thus increasing bone toughness. The SEM and FEM results provided in this paper could suggest that the bone resistance to fracture can best be represented by a parameter describing osteonal density. This paper, through observation of the microcrack propagation trajectory, expands the results of Yeni *et al.* [37], where the relationship between improvements in fracture toughness in modes I & II, and human femur osteon density is reported.

The SEM photographs from fracture surface shows that, if the direction of the pre-crack is perpendicular to fibres, the crack deviates and takes a path between the fibres. This result is in accordance with previous observations [38]. Our current and previous FEM models fail to study such phenomena as delamination and cement line debonding [18]. However SEM observation of fracture surface at inter-lamellar and microstructural level shows that matrix deformation, delamination and cement line debonding are the factors which dominate the final fracture, each of which absorb some of the energy prior to final failure [39]. It can therefore be anticipated that the sum of energy absorbed by these phenomena increases the fracture toughness of cortical bone.

Conclusion

Material properties and morphological parameters of the microstructure greatly influence the fracture behavior of bone. This report emphasizes the effect of tissue properties differences upon fracture phenomena. The effect of osteons on microcrack trajectories and increased bone toughness are of particular novelty and interest.

References

- Launey ME, Buehler MJ, Ritchie RO (2010) On the Mechanistic Origins of Toughness in Bone. Annual Review of Materials Research 40: 25-55.
- Ritchie RO, Buehler MJ, Hansma P (2009) Plasticity and toughness in bone. Physics Today 62:41-47.
- Diab T, Vashishth D (2007) Morphology, localization and accumulation of *in vivo* microdamage in human cortical bone. Bone 40:612-618.
- Hui SL, Slemenda CW, Johnston CC (1988) Age and bone mass as predictors of fracture in a prospective-study. Journal of Clinical Investigation 81:1804-1809.
- Heaney RP (2005) Is the paradigm shifting? Bone 35:457-465.
- Parfitt AM (1987) Boneremodeling and bone loss – Understanding the pathophysiology of osteoporosis. Clinical Obstetrics and Gynecology 30:789-811.
- Kanis JA, Melton LJ, Christiansen C, Johnston CC, Khaltaev N (1994) Prospective – The diagnosis of osteoporosis. Journal of Bone and Mineral Research. 9:1137-1141.
- McCabe F, Zhou LJ, Steele CR, Marcus R (1991) Noninvasive assesment of ulnar bending stiffness in women. Journal of Bone and Mineral Research 6:55-59.
- Weiner S, Wagner HD (1998) The material bone: Structure mechanical function relations. Annual Review of Materials Science 28:27-98.
- Fratzl P, Weinkamer R (2007) Nature's hierarchical materials. Progress in Materials Science 52:1263-1334.
- Zimmermann EA, Launey ME, Ritchie RO (2010) The significance of crack-resistance curves to the mixed-mode fracture toughness of human cortical bone. Biomaterials 31:5297-5305.
- Yang QD, Cox BN, Nalla RK, Ritchie RO (2006) Fracture length scales in human cortical bone: The necessity of nonlinear fracture models. Biomaterials 27: 2095–2115.
- Guo XR, Liang LC, Goldstein SA (1998) Micromechanics of osteonal cortical bone fracture. Journal of Biomechanical Engineering 120: 112-117.
- O'Brien FJ, Taylor D, Lee TC (2005) The effect of bone microstructure on the initiation and growth of microcracks. Journal of Orthopaedic Research 23: 475-480.
- Huang J, Rapoff AJ, Haftka RT, (2006) Attracting cracks for arrestment in bone-like composites. Materials and Design 27: 461–469.
- Raeisi Najafi A, Arshi AR, Eslami MR, Fariborz S, Moeinzadeh M (2007) Haversian cortical bone model with many radial microcracks: An elastic analytic solution. Medical Engineering & Physics 29: 708–717.
- Raeisi Najafi A, Arshi AR, PourAkbar Saffar K, Eslami MR, Fariborz S, Moeinzadeh MH, (2009) A fiber-ceramic matrix composite material model for osteonal cortical bone fracture micromechanics: Solution of arbitrary microcracks interaction. Journal of the Mechanical Behavior of Biomedical Materials 2: 217-223.
- Raeisi Najafi A, Arshi AR, Eslami MR, Fariborz S, Moeinzadeh M (2007) Micromechanics fracture in osteonal cortical bone: A study of the interactions between microcrack propagation, microstructure and the material properties. Journal of Biomechanics 40: 2788-2795.
- Rho JY, Pharr GM (1999) Effects of drying on the mechanical properties of bovine femur measured by nanoindentation. Journal of Materials Science – Materials in Medicine 10:485-488.
- Hogan HA (1992) Micromechanics modeling of Haversian cortical bone properties. Journal of Biomechanics 25:549-556.
- Burr DB, Schaffler MB, Fredericson RG (1988) Composition of the cement line and its possible mechanical role as a local interface in human compact bone. Journal of Biomechanics 21:939-945.
- Curry J (1984) The mechanical adaptations of bones. New York: Princeton University Press.
- Advani SH, Lee TS, Martin RB (1987) Analysis of crack arrest by cement lines in osteonal bone; in: Erdman AG (ed. 1987) Advances in Bioengineering, New York: ASME. 57-88.
- Zedda M, Lepore G, Manca P, Chisu V, Farina V (2008) Comparative bone histology of adult horses (*Equus caballus*) and cows (*Bos taurus*). Anatomia Histologia Embryologia 37:442-445.
- Chen PY, Stokes AG, McKittrick J (2009) Comparison of the structure and mechanical properties of bovine femur bone and antler of the north american elk (*Cervus elaphus canadensis*). Acta Biomaterialia 5:695-706.
- Burket J, Gourion-Arsiquaud S, Havill LM, Baker SP, Boskey AL, van der Meulen MCH (2011) Microstructure and nanomechanical properties in osteons relate to tissue and animal age. Journal of Biomechanics 44 (2):277-284.
- Dixon KJ, Novak SA, Robbins G, Schablitsky JM, Scott GR, Tasa GL (2010) Men, women, and children starving:

- Archaeology of the donner family camp. *American Antiquity* 75:627-656.
28. Skedros JG, Mason MW, Bloebaum RD (1994) Differences in osteonal micromorphology between tensile and compressive cortices of a bending skeletal system – Indications of potential strain – specific differences in bone microstructure. *Anatomical Record* 239:405-413.
 29. Locke M (1995) Structure of long bones in mammals. *Journal of Morphology* 262:546-565.
 30. Schaffler MB, Choi K, Milgrom C (1995) Aging and matrix microdamage accumulation in human compact bone. *Bone* 17: 521-525.
 31. Phelps JB, Hubbard GB, Wang X, Agrawal CM (2000) Microstructural heterogeneity and the fracture toughness of bone. *Journal of Biomedical Material Research* 51: 735-741.
 32. Doblaré M, García JM, Gómez MJ (2004) Modeling bone tissue fracture and healing: a review. *Engineering Fracture Mechanics* 71: 1809-1840.
 33. Crofts R.D, Byoce TM, Milgrom C (1994) Aging changes in osteon mineralization in the human femoral neck. *Bone* 15: 137-152.
 34. Mohsin S, O'Brien FJ, Lee TC (2006) Osteonal crack barriers in ovine compact bone. *Journal of Anatomy* 208: 81-89.
 35. Schaffler MB, Pitchford WC, Choi K, Riddle JM (1994) Examination of compact bone microdamage using back-scattered electron microscopy. *Bone* 15: 485-488.
 36. Akkus O & Rimnac CM (2001) Cortical bone tissue resists fatigue fracture by deceleration and arrest of microcrack growth. *Journal of Biomechanics* 34: 757-764.
 37. Yeni YN, Brown CU, Wang Z, Norman TL (1997) The influence of bone morphology on fracture toughness of the human femur and tibia. *Bone* 21: 453-459.
 38. Behiri JC, Bonfield W (1989) Orientation dependence of the fracture mechanics of cortical bone. *Journal of Biomechanics* 22:865-872.
 39. Braidotti P, Branca FP, Stagni L (1997) Scanning electron microscopy of human cortical bone failure surface. *Journal of Biomechanics* 30: 155-162.